





Article

pubs.acs.org/acssensors

# Natural Perspiration Sampling and in Situ Electrochemical Analysis with Hydrogel Micropatches for User-Identifiable and Wireless Chemo/Biosensing

- 4 Shuyu Lin, † Bo Wang, † Yichao Zhao, † Ryan Shih, † Xuanbing Cheng, † Wenzhuo Yu, † Hannaneh Hojaiji, † Haisong Lin, † Claire Hoffman, † Diana Ly, † Jiawei Tan, † Yu Chen,
- 6 Dino Di Carlo, Carlos Milla, and Sam Emaminejad\*,†,||
- 7 †Department of Electrical and Computer Engineering, ‡Department of Materials Science and Engineering, §David Geffen School of
- 8 Medicine, Department of Bioengineering, and Molecular Instrumentation Center, University of California, Los Angeles,
- 9 California 90095, United States
- 10 #The Stanford Cystic Fibrosis Center, Center for Excellence in Pulmonary Biology, Stanford School of Medicine, Palo Alto,
- 11 California 94305, United States
  - Supporting Information

13

14

1.5

16

17

18

19

20

21 22

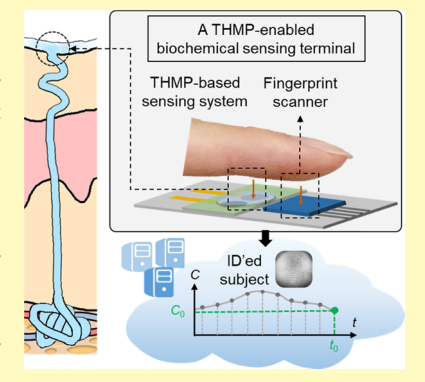
23

24

2.5

26

27 28 ABSTRACT: Recent advances in microelectronics, microfluidics, and electrochemical sensing platforms have enabled the development of an emerging class of fully integrated personal health monitoring devices that exploit sweat to noninvasively access biomarker information. Despite such advances, effective sweat sampling remains a significant challenge for reliable biomarker analysis, with many existing methods requiring active stimulation (e.g., iontophoresis, exercise, heat). Natural perspiration offers a suitable alternative as sweat can be collected with minimal effort on the part of the user. To leverage this phenomenon, we devised a thin hydrogel micropatch (THMP), which simultaneously serves as an interface for sweat sampling and a medium for electrochemical sensing. To characterize the performance of the THMP, caffeine and lactate were selected as two representative target molecules. We demonstrated the suitability of the sampling method to track metabolic patterns, as well as to render sample-to-answer biomarker data for personal monitoring (through coupling with an



electrochemical sensing system). To inform its potential application, this biomarker sampling and sensing system is incorporated within a distributed terminal-based sensing network, which uniquely capitalizes on the fingertip as a site for simultaneous biomarker data sampling and user identification.

29 **KEYWORDS:** natural perspiration, hydrogel micropatch, biosensor, sample identification, electrochemical analysis, Internet-of-Things, lactate, caffeine

ecent advances in miniaturized electronics, microfluidics, and electrochemical sensing platforms have paved the 33 path for the realization of chemo/biosensing networks geared 34 toward general population health and wellness monitoring. 1-35 To this end, a sweat-based sensing modality presents a great 36 potential for the integration into such networks, as it provides 37 noninvasive access to molecular-level information, enabling 38 insight into the body's dynamic chemistry. 5-7 However, 39 realizing effective sweat sampling remains a fundamental 40 challenge in noninvasive chemo/biosensing. Previous studies 41 have mainly relied on either physical or chemical stimulation 42 procedures (e.g., exercise, 9,10 heat, 11 and iontophoresis 12) to 43 induce sweat production in substantial volumes ( $\sim$ 50  $\mu$ L). 44 While useful for infrequent analysis in laboratory settings, 45 challenges remain when implementing these methods in the 46 context of (semi)continuous measurements: exercise requires 47 strenuous physical activity, which may not be suitable for all 48 potential users (especially the bedridden, neonatal, or elderly 49 populations); heat can lead to exhaustion and discomfort,

which could cause noncompliance if used in a device for 50 patients; and iontophoresis has numerous challenges related to 51 the integration of device- and circuit-level stimulating 52 components, which are currently being addressed. It is also 53 worth noting that the analyte concentration in sweat has been 54 shown to be sweat gland secretory rate-dependent, which, in 55 the absence of corrective calibration mechanisms, leads to 56 distortion in the biomarker measurements when relying on 57 stimulation-based sweat sampling.

Given the challenges of these sampling methods, alternative 59 methods of accessing sweat biomarkers may warrant 60 exploration. One such alternative is naturally occurring/ 61 background thermoregulatory perspiration (hereinafter, re- 62 ferred to as natural perspiration). Natural-perspiration-based 63

Received: September 4, 2019 Accepted: November 8, 2019

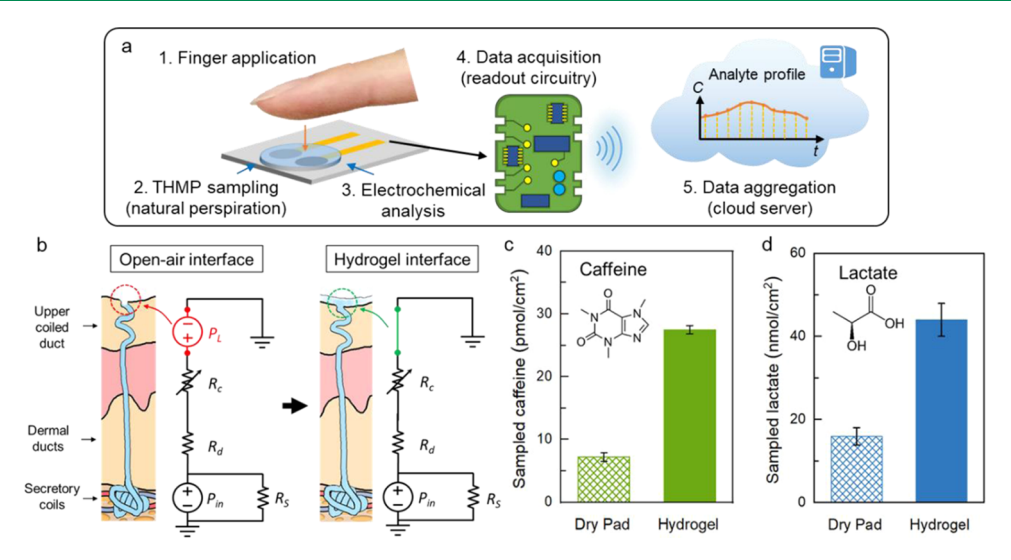


Figure 1. (a) Schematic of the THMP-based naturally perspired analyte sampling and wireless in situ electrochemical analysis on a fingertip. (b) First-order microfluidic model for natural perspiration sampling with an open-air interface and hydrogel interface. (c, d) Amount of caffeine (c) and lactate (d) sampled per unit area on the fingertips with a dry absorbent pad (can be effectively considered as an open-air sampling interface) and hydrogel interface (sampled from four different fingers of the same subject; error bars indicate standard error). Sampling events targeting caffeine were conducted 2 h after the consumption of beverages containing 150 mg caffeine.

64 sampling eliminates the need for active stimulation and 65 provides a stable secretion rate (on the order of 1 nL/min 66 per gland) within the time window of sampling. 13 This 67 minimizes the confounding effect of sweat rate variability and 68 leads to more accurate analysis. Furthermore, owing to its low 69 secretion rate, natural perspiration is speculated to give 70 adequate time for the low-membrane-permeability analytes to 71 partition from blood to sweat, and thus sweat-blood 72 correlation can be established for a wider range of 73 biomarkers. 15,16 While this phenomenon has not been widely 74 used for bioanalytical device development, academic forensic 75 science studies have already demonstrated its utility in residual 76 fingerprint analysis for the simultaneous rendering of 77 biochemical and user identification information. 17 In one 78 respect, drugs or metabolites of target compounds can be 79 extracted from the sweat, yielding information about the 80 individual's consumption of illicit substances with the added 81 potential to make inferences regarding the individual's general 82 health state. 18 Complementarily, the spatial distribution of 83 those extracted analytes, coupled with ridge and groove 84 patterns of the sweat left on the surface, can be exploited to 85 produce a latent fingerprint image to uniquely identify the 86 individual. 19

To fully realize the potential of natural perspiration for noninvasive health monitoring applications, two fundamental challenges related to biomarker sampling and sensing must be addressed. First, instantaneously secreted sweat droplet sampling is challenging because of its low flow rate and associated volume of secretion, and such sampling requires sweat collection by accumulation over a period of time in suitable interfaces/reservoirs to facilitate effective analyte partitioning and collection from sweat glands. Second, in situ electrochemical techniques (which are commonly used for sweat analysis at the "point-of-person") require a reliable medium to envelop and protect sensing electrodes, as well as 99 facilitate analyte transport to those electrodes for detection.

Previous work demonstrating analyte sampling interfaces for natural perspiration from the skin can generally be categorized by interface type (either dry or wet). Dry interfaces (like

unwetted filter paper or the commercial PharmChek skin 103 patches) typically require longer collection periods (on the 104 order of days) and are thus more useful in obtaining a binary 105 presence metric indicating if a compound has accumulated to 106 sufficient levels for detection. Hydrated interfaces (like 107 wetted filter paper or hydrogels), on the other hand, are better 108 suited for health monitoring devices and terminals aiming to 109 study and characterize pharmacokinetic and metabolic profiles 110 of the subjects due to their shorter sampling times and 111 improved partitioning efficiency (greater analyte collec- 112 tion). 22-24 Both interface types, however, are commonly 113 used only as reservoirs for subsequent analysis in a decoupled 114 manner with bulky laboratory instruments (e.g., mass 115 spectrometers). Recently, a proof-of-concept of lactate 116 measurement with a sensor-coupled hydrogel was demon- 117 strated for fingertip sweat sampling; 25 however, the key 118 hydrogel sensor performance metrics (including the sensor's 119 limit of detection (LoD), detection range, and selectivity) has 120 not been fully characterized, and its deployment in diverse 121 application spaces has not been demonstrated.

Here, we devise a thin hydrogel micropatch (THMP) for 123 simultaneous natural perspiration collection and in situ 124 electrochemical analysis (Figure 1a) and then demonstrate 125 f1 its utility in an integrated health monitoring setting to illustrate 126 its enabling potential in diverse application spaces. To 127 characterize THMP's performance, caffeine and lactate were 128 selected as two representative target molecules. The choice of 129 caffeine was motivated by its therapeutic potential for the 130 treatment of airway obstruction and apnea of prematurity 26,27 131 and the fact that it is a xenobiotic. We particularly exploit its 132 xenobiotic nature to perform controlled studies for determin- 133 ing optimal sampling conditions and demonstrating the utility 134 of the approach for tracking dosage levels and metabolic 135 patterns. The choice of lactate was motivated by its clinical 136 significance in a variety of applications<sup>28</sup> and the fact that 137 lactate-targeting sensors have been extensively explored for 138 sweat analysis. 29,30 Accordingly, by coupling a custom- 139 developed wireless enzymatic lactate sensing module with 140 the hydrogel interface, we demonstrate a THMP-based sensing 141

142 system, which noninvasively renders sample-to-answer bio-143 marker data from the fingertip. Furthermore, this coupled 144 system was leveraged to demonstrate the proof-of-concept of a 145 distributed terminal-based chemo/biosensor network, which 146 uniquely capitalizes on the fingertip as a site for simultaneous 147 biomarker data sampling and user identification. This terminal-148 based sensing modality can be embedded within the extant and 149 future Internet-of-Thing (IoT) infrastructures for community-150 based health monitoring.

#### 51 EXPERIMENTAL SECTION

Materials and Reagents. Agarose, sodium acetate buffer solution 153 (3 M, pH = 5.2  $\pm$  0.1), caffeine, caffeine- $^{13}$ C<sub>3</sub> (1 mg/mL in 154 methanol), multiwalled carbon nanotube (MWCNT, carboxylic acid-155 functionalized), Nafion perfluorinated resin solution (5 wt %). 156 chloroplatinic acid hexahydrate (H<sub>2</sub>PtCl<sub>6</sub>·6H<sub>2</sub>O), m-phenylenedi-157 amine, bovine serum albumin (BSA), glutaraldehyde solution (25 158 wt %), poly(vinyl chloride) (PVC), tetrahydrofuran (THF), sodium 159 L-lactate, D-glucose, uric acid (UA), ascorbic acid (AA), sodium 160 chloride (NaCl), and potassium chloride (KCl) were purchased from 161 Sigma-Aldrich (Missouri). 2-Propanol (IPA), water (Optima LC/MS 162 grade), formic acid, acetonitrile (Optima LC/MS grade), and 163 phosphate-buffered saline (PBS, pH = 7.4) were purchased from 164 Fisher Scientific (Massachusetts). Silver-silver chloride (Ag/AgCl) 165 ink was purchased from Ercon Incorporated (Massachusetts). Lactate 166 oxidase (LOx) was purchased from Toyobo USA, Inc. (New York). Molecular weight cutoff (MWCO, 10 kDa) centrifugal filters (Amicon Ultra-0.5) were purchased from Sigma-Aldrich. Double-169 sided tape (170 µm thick, 9474LE 300 LSE) was purchased from 3M 170 Science (Minnesota). Poly(ethylene terephthalate) (PET, 100  $\mu$ m 171 thick) was purchased from MG Chemicals (BC, Canada). CF1 172 absorbent pads were purchased from GE Healthcare Bio-Sciences (Pennsylvania). Espresso containing 75 mg caffeine per shot used for caffeine testing in human subjects was purchased from Peet's Coffee 174

THMP Fabrication. The THMPs were prepared using a layered 176 177 mold assembly of a glass slide substrate, a middle layer consisting of 178 one or more strips of double-sided tape, and a PET capping layer 179 (Figure S1). Tape and PET layers were laser-cut to form a 180 microfluidic chamber and access ports, respectively (Epilog Mini 181 24, Epilog Laser). The chamber (6 mm in diameter) was used to 182 define the hydrogel patch size, and 1 mm inlet and outlet ports in the 183 PET layer enabled solution injection into the chamber. Hydrogel 184 thickness was controllably adjusted by varying the number of double-185 sided tape strips used to create the wall of the microfluidic chamber. 186 Hydrogel (containing 2% agarose) was then prepared by dissolving 187 agarose powder in a 0.01 M acetate buffer (diluted from a 3 M stock solution, pH = 5, similar to sweat<sup>31</sup>) followed by placing the resulting 189 mixture in an 80 °C water bath. After agarose was completely 190 dissolved, the solution was immediately injected into the preas-191 sembled mold (heated to 80 °C on a hot plate). Following sufficient 192 cooling, the fabricated hydrogel patch was obtained by peeling the 193 tape and PET layers from the glass slide. Patch volumes were 194 calculated from weight measurements assuming a density of 1 g/mL. Natural Perspiration Sampling. For natural perspiration 195 196 sampling intended for caffeine analysis, participants with a regular caffeine intake (e.g., routine or daily consumption of caffeinated beverages) were excluded to avoid confounding factors (e.g., caffeine 199 accumulation in body), 32 and all of the participants were required to 200 abstain from the consumption of food, beverages, and drugs 201 containing caffeine for 24 h prior to the experiment. The skin sampling regions of interest were washed with hand soap sheets (Travelon, Illinois) and deionized (DI) water followed by wiping with 204 Kimwipes containing 70% IPA. The efficiency of the adopted cleaning 205 protocol is demonstrated in Figure S2. A THMP or absorbent pad 206 was placed on the skin for 5 min for sweat sampling, and a 207 polyethylene plastic film was used to cover the device to avoid 208 evaporation. Given that the natural perspiration rate, on the high end,

is on the order of  $0.4 \, \mathrm{mg/(cm^2 \, min)^{33}}$  (which is much higher than the 209 rate of observed transepithelial water loss <sup>34</sup>), the incremental volume 210 contribution of natural perspiration to the THMP is less than 1  $\mu$ L. As 211 the original THMP volume is  $\sim 8 \, \mu$ L, the volumetric contribution by 212 natural perspiration results in dilution by a factor of  $\sim 10$ , allowing to 213 establish a linear relationship between the collected analyte amount 214 and the corresponding analyte concentration in perspiration.

**Lactate Quantification with Lab Instrument.** After natural 216 perspiration sampling, the THMP or absorbent pad was placed into 217 an Eppendorf tube containing  $100~\mu L$  of acetate buffer (0.01 M, pH = 218 5), and the tube was sonicated for 5 min at room temperature for the 219 extraction of the target molecules. The lactate concentration in the 220 tube was quantified directly with the YSI 2900 analyzer (YSI 221 Incorporated, Ohio) in duplicate, and the average value was used. The 222 amount of lactate sampled per unit area was determined from the 223 concentrations in the extraction buffer, extraction buffer volume, and 224 the area of the THMP or absorbent pad.

Caffeine Quantification with Liquid Chromatography- 226 Tandem Mass Spectrometry (LC-MS/MS). The amount of 227 caffeine sampled with the THMP or absorbent pad was measured 228 by LC-MS/MS with multiple reaction monitoring (MRM) technique 229 (Figure S2). <sup>13</sup>C isotopically labeled caffeine (caffeine-<sup>13</sup>C<sub>3</sub>) was 230 used as the internal standard (IS). For calibration, different 231 concentrations of caffeine were spiked into water (Optima LC/MS 232 grade) to make standard solutions of 0.0, 1.0, 2.0, 5.0, 10.0, 50.0, 233 100.0, and 200.0 nM. For the analysis of real samples, the 234 perspiration-sampled THMP or absorbent pad was placed into an 235 Eppendorf tube containing 200  $\mu$ L of acetate buffer (0.01 M, pH = 5), 236 and the tube was sonicated for 5 min at room temperature for target 237 molecule extraction. A molecular-weight cutoff (MWCO) filtering 238 was used to remove any particulate matter from the sample. The 239 standard solution or real sample extraction of 150  $\mu$ L was mixed with 240 1.5  $\mu$ L of 10.0  $\mu$ M IS (to reach a final IS concentration of 0.1  $\mu$ M), 241 loaded into a 10 kDa MWCO filter, and centrifuged at 14 000g for 10 242 min. The low-molecular-weight filtrate was then transferred into an 243 autosampler vial for caffeine quantification.

An Agilent 1200 series HPLC (Agilent Technologies, California) 245 equipped with a HTS PAL autosampler (CTC Analytics, Minnesota) 246 was coupled to an API 4000 triple quadrupole mass spectrometer 247 (Sciex, ON, Canada) for MRM experiments. A Zorbax 300 SB-C18 248 column (0.5 ID  $\times$  150 mm L, 5  $\mu$ m, Agilent Technologies) was used 249 for separation. Solvent A was water with 0.1% formic acid, and solvent 250 B was acetonitrile with 0.1% formic acid. The flow rate was 400  $\mu$ L/ 251 min with the following gradient: 5% B (0–0.5 min), from 5 to 90% B 252 (0.5–5.5 min), 90% B (5.5–8.5 min), from 90 to 5% B (8.5–9.0 253 min), 5% B (9.0–11.0 min). Sample vials were maintained at 4 °C in 254 the autosampler tray. A sample of 20  $\mu$ L was loaded onto the column 256 each time.

The instrument was operated in an MRM mode with the following 257 m/z transitions: 195.2  $\rightarrow$  138.1 for caffeine and 198.1  $\rightarrow$  140.1 for 258 caffeine— $^{13}$ C<sub>3</sub>. The declustering potential (DP), entrance potential 259 (EP), collision energy (CE), and collision cell exit potential (CXP) 260 were optimized at 71, 10, 27, and 8 V for caffeine, and 86, 10, 27, and 261 8 V for caffeine— $^{13}$ C<sub>3</sub>, respectively. Ion spray voltage and temperature 262 were 5500 V and 400 °C, respectively. The collision gas, curtain gas, 263 and ion source gas 1 and 2 were set at 4, 30, 30, and 50 psi, 264 respectively.

**Lactate Sensing Module Fabrication.** The lactate sensing 266 module was fabricated on a pair of gold (Au) electrodes (diameter: 267 2.4 mm, 20 nm Cr/100 nm Au) deposited and patterned on the PET 268 substrate. The reference electrode was fabricated by drop-casting the 269 Ag/AgCl ink directly on the Au electrode followed by baking at 80 °C 270 for 10 min. To fabricate the working electrode, 1.15  $\mu$ L of the 271 MWCNT solution (2 mg/mL in a 5 wt % Nafion solution) was drop-272 cast onto the Au electrode and dried at an ambient environment. 273 Platinum nanoparticles (PtNPs) were then electrochemically 274 deposited onto the MWCNT-modified Au electrode in the PtNP 275 deposition solution (2.5 mM H<sub>2</sub>PtCl<sub>6</sub> and 1.5 mM formic acid in DI 276 water) using cyclic voltammetry (0—1.0 V vs Ag/AgCl, 20 cycles, 50 277 mV/s). The poly-m-phenylenediamine (PPD) layer was subsequently 278

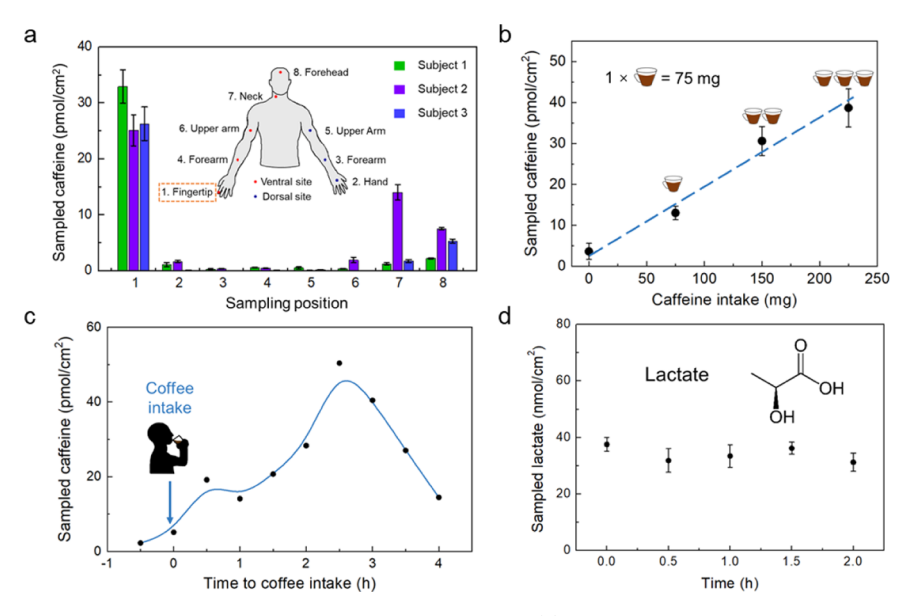


Figure 2. Characterization of naturally perspired analyte sampling with THMP. (a) Amount of caffeine sampled per unit area on different body sites (three subjects with three trials at each position; sampled 2 h after the consumption of a beverage containing 150 mg of caffeine; error bars indicate standard error). (b) Amount of caffeine sampled per unit area on the fingertips of the same subject with different caffeine dosages (sampled from three different fingers, 2 h after the consumption of beverages with the annotated caffeine content; error bars indicate standard error). (c) Amount of caffeine sampled per unit area on the fingertips of a single subject at 30 min intervals before and after the consumption of a beverage containing 150 mg of caffeine. (d) Amount of lactate sampled per unit area on the fingertips at 30 min intervals (from a sedentary subject, sampled from three different fingers; error bars indicate standard error).

279 electrochemically deposited onto the Au/MWCNT/PtNP electrode 280 with the m-phenylenediamine solution (5 mM in PBS) by applying 281 0.85 V (vs Ag/AgCl) for 120 s. The modified working electrode was 282 then washed with DI water and dried. To immobilize LOx, BSA was 283 used as a stabilizer and glutaraldehyde was used as a cross-linker. 284 Specifically, 500  $\mu$ L of the BSA solution (10 mg/mL in PBS) was first 285 mixed with 4  $\mu$ L of glutaraldehyde solution (25 wt %), followed by 286 mixing with the lactate oxidase solution (10 mg/mL in PBS) at a 1:1 287 ratio (v/v). The enzyme mixture (1.15  $\mu$ L) was drop-cast onto the 288 Au/MWCNT/PtNP/PPD electrode and dried at room temperature. 289 Then, the sensor was dip-coated with the PVC solution (3 wt % in 290 THF) twice and dried at 4 °C in a dark environment overnight. The 291 fabricated sensors were stored at 4 °C.

Lactate Sensing Module Characterization and Measure-293 ment. The thickness of each layer of the lactate sensor was measured 294 by the Dektak 6M profilometer. To characterize the electrochemical performance of the developed lactate sensing module, constant 296 potential amperometric measurements were conducted at +0.5 V vs 297 Ag/AgCl. By drop-casting the lactate solution (in PBS, pH = 7.4) of 298 different concentration levels onto the corresponding sensors, 299 calibration plots were obtained, which were utilized to determine 300 the performance of the developed sensing interface. The limit of detection (LoD) for each amperometric sensing interface was 302 calculated as LoD =  $3 \times SD/slope$ , where SD is the standard deviation of the baseline noise in the PBS, and the slope is defined as 303 the amperometric current change vs lactate concentration change. Sensitivity is calculated as the slope divided by the sensor's surface 306 area. To characterize the THMP-based sensing module, the THMPs were soaked in the analyte solution (in PBS, pH = 7.4) for at least 10 308 min and then transferred onto the sensor surface (while ensuring that minimal lactate solution residue was present on the surface of the 310 THMP). Corresponding amperometric measurements were con-311 ducted after placing the presoaked THMP onto the sensor. Lactate 312 tracking on the fingertips was performed by instructing the subject to press the index fingertip onto the THMP for 5 min, followed by 314 taking an amperometric measurement upon the removal of the 315 fingertip.

Readout Circuit Module for THMP-Based Wireless Sensing
System. The wireless amperometric measurement was realized with a

miniaturized readout circuitry similar to our previous effort... The 318 circuitry includes an ultralow-power microcontroller unit (MCU, 319 STM8L-UFQFN20, STMicroelectronics, California), which is inter- 320 faced with an onboard Bluetooth transceiver to wirelessly and 321 bilaterally communicate user commands and the sensor's output 322 current in real time with a custom-developed smartphone application. 323 The MCU controls the developed analog signal acquisition and 324 conditioning circuits interfacing the THMP-based sensing module. An 325 onboard potentiostat chip (LMP91000, Texas Instruments, Texas) 326 was programmed to apply +0.5 V across the working and the 327 reference electrodes and set to convert the acquired current signal to 328 voltage values with the aid of its internal transimpedance amplifier. 329 The corresponding output voltage was filtered by a fifth-order low- 330 pass filter module (MAX7422 chip, cutoff frequency: 1 Hz, Maxim 331 Integrated, California) and converted into the digital domain by a 12- 332 bit analog-to-digital unit (built-in in the MCU). A compact 333 rechargeable lithium-ion polymer battery with a nominal voltage of 334 3.7 V and a capacity on the order of 100 mAh was used to power the 335

**User Identification Module.** The fingerprints of the users were 337 collected and identified with a commercial fingerprint scanner 338

module (TTL GT-511C1R, SparkFun Electronics, Colorado), 339 which bilaterally communicates with a microcontroller (Atmega8) or 340 the provided software. The fingerprint templates of all of the users 341 were stored in the fingerprint scanner module before identification 342 tests.

Institutional Review Board (IRB) Approval for Human 344 Subject Testing. The conducted human subject experiments were 345 performed in compliance with the protocols that have been approved 346 by the IRB at the University of California, Los Angeles (IRB #17- 347 000170). All subjects gave written informed consent before 348 participation in the study.

# ■ RESULTS AND DISCUSSION

**Naturally Perspired Analyte Sampling.** To set up a 351 framework for natural-perspiration-based analyte sampling, we 352 expand upon the first-order microfluidic models of eccrine 353 sweat glands presented in the previous studies... <sup>16</sup> As shown in 354

350

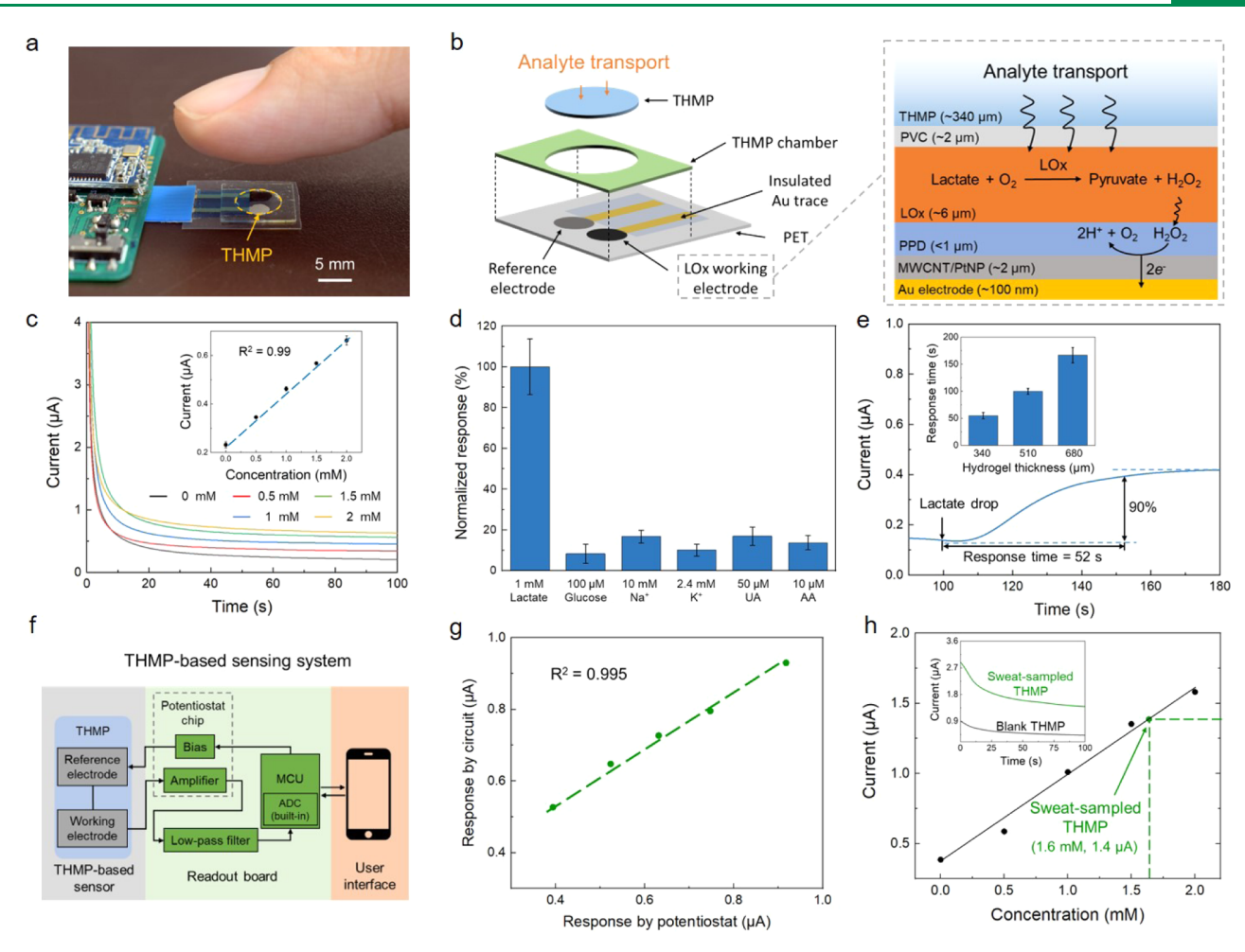


Figure 3. (a) Image of a one-touch THMP-based wireless electrochemical sensing system (sampling from a fingertip). (b) Schematic of the THMP-based lactate sensing module. Zoomed view (right) shows the structure of the LOx working electrode (with the approximate thickness of each layer annotated). (c) Measured amperometric responses of THMP-based lactate sensing module upon the placement of hydrogels presoaked in solutions with different lactate concentration levels. The inset shows the corresponding calibration curve (error bars indicate standard error, measured with three different THMPs). (d) Selectivity study of THMP-based lactate sensing module. The tests were performed separately, with THMPs presoaked in solutions containing different interfering species. Measured amperometric responses were normalized to a 1 mM lactate readout (error bars indicate standard error, n = 3). (e) Dynamic THMP-based amperometric response to 1  $\mu$ L of a 10 mM sodium lactate concentrated solution, drop-cast onto a 340  $\mu$ m-thick blank hydrogel. The inset shows the response time vs hydrogel thickness (error bars indicate standard error, n = 3). (f) System-level block diagram of the THMP-based wireless sensing system (interfaced with a readout board and a mobile application). (g) Amperometric response of a THMP-based lactate sensor measured by the developed readout circuitry vs potentiostat. (h) Representative measurement (1.4  $\mu$ A) derived from the placement of the fingertip on the integrated sensing system, determining the sampled lactate concentration to be 1.6 mM (upon postcalibration). The nset shows the raw recording of the corresponding measurement, as well as the recording for the case of a blank THMP (included for comparison).

355 Figure 1b, P<sub>in</sub> is the varying hydrostatic-osmotic pressure (originating from the accumulation of Na<sup>+</sup> and Cl<sup>-</sup> ions in the secretory lumen<sup>35</sup>), which pumps sweat from the glands to the pores on the skin surface, forming sweat droplets. R<sub>c</sub>, R<sub>d</sub>, and  $R_{\rm s}$  are the fluidic resistances of the upper coiled duct, the 360 dermal duct, and the secretory coil, respectively. The surface-361 tension-induced Laplace pressure, P<sub>L</sub>, acts to oppose sweat secretion, where the surface tension corresponds to that of a sweat droplet with a finite radius of curvature forming on the surface of the skin. For natural perspiration to occur,  $P_{in}$  must  $_{365}$  be increased beyond  $P_{\rm L}$ . Once perspiration has occurred,  $P_{\rm in}$ 366 will be reduced (due to the loss of the accumulated Na<sup>+</sup> and 367 Cl<sup>-</sup> ions upon secretion) and must rise above the  $P_L$  threshold 368 again to induce the next cycle of the sweat secretion, giving rise 369 to the pulsatile behavior of natural perspiration. This behavior 370 is consistent with the previous observations 16 and our own 371 examination of natural perspiration (Supporting Information

Movie 1, a video recording of a subject's fingertip), where the 372 naturally perspired droplets were generated and then 373 evaporated.

To eliminate the  $P_{\rm L}$  pressure barrier, a hydrogel-based 375 collection interface is devised. By creating a continuous 376 hydrophilic fluidic path connecting the secretory coil and 377 sampling reservoir, the hydrogel effectively reduces  $P_{\rm L}$  to zero 378 (Figure 1b, right). In this way, even a small  $P_{\rm in}$  buildup will 379 result in sweat secretion that can be utilized for analyte 380 collection by the hydrogel. In addition, due to its aqueous 381 nature, the hydrogel interface also serves to facilitate the 382 diffusion of analytes from sweat to the reservoir. These two 383 features render the hydrogel an effective collection reservoir for 384 capturing analyte flux. To illustrate the analyte collection 385 efficacy of the devised THMP, perspiration sampling experi-386 ments targeting caffeine and lactate (as two representative 387 molecules) were performed. The caffeine sampling experi-388

389 ments were performed 2 h after the consumption of caffeinated 390 beverages. The analyte collection capability of the THMP was 391 compared with that of the dry absorbent pad (which can be 392 effectively considered as an open-air sampling interface in the 393 described model, laser-cut to be the same size as the THMP). 394 For each target, the two sampling media were placed side by 395 side on a subject's fingertip. After sampling, the two media 396 were immersed in acetate buffer solutions for analyte extraction 397 followed by quantification. Caffeine concentration levels were 398 measured by LC-MS/MS (similar to previous effort,; 36,37 399 calibration shown in Figure S3), and lactate concentration 400 levels were measured by a YSI analyzer. The analyte sampling 401 characterization results for both molecules indicated that the 402 hydrogel interface sampled approximately three times as much 403 analytes as the dry pad interface (Figure 1c,d), which is in 404 agreement with the described first-order model and informs 405 the enhanced analyte collection capability of the THMP.

To further validate the suitability of THMP for analyte 407 sampling, it was deployed on eight different body sites for caffeine sampling on three subjects. Figure 2a shows that the 409 hydrogel micropatch was able to collect detectable (by LC-410 MS/MS) levels of xenobiotics for most of the sampling points. 411 In particular, for all of the subjects, the highest amounts of 412 analytes (per unit area) were collected from the

fingertips among the investigated body sites. This observa-414 tion may be attributed to the fact that the fingertips have the 415 highest density of eccrine sweat glands<sup>38</sup> and/or that blood 416 capillaries lie in close proximity to the fingertip's sweat 417 glands. <sup>39</sup> From this investigation, the fingertips were 418 determined to be the optimal site for sampling due to their 419 higher analyte yield, and thus this site was used to conduct the 420 subsequent analyte collection characterization experiments.

To illustrate the utility of the THMP for natural perspiration 422 sampling, we demonstrated its capability to track different 423 caffeine intake dosage levels in a subject. Accordingly, the 424 subject was instructed to consume caffeine-based beverages 425 with four different caffeine amounts (0, 75, 150, and 225 mg), 426 and at least 24 h of washout period was included in between to 427 avoid the carryover effect. THMP-based sampling was 428 performed 2 h after each caffeine intake. As shown in Figure 429 2b, the quantification results indicate that the amount of 430 caffeine sampled in the hydrogel increased linearly with 431 increasing dosage, which, in turn, illustrates the reliability of 432 the THMP-based sampling method. Furthermore, we 433 employed THMP to characterize the temporal metabolic 434 pattern of caffeine (as a xenobiotic). Accordingly, THMP-435 based sampling on a subject's fingertip was performed at 30 436 min intervals before and after the consumption of a beverage 437 containing 150 mg of caffeine. As shown in Figure 2c, for this 438 subject, the sampled caffeine peaked around 2.5 h after caffeine 439 intake followed by a steady decline. Similar experiments with 1 440 h sampling intervals were also conducted for three additional 441 subjects, where the captured caffeine metabolic patterns 442 (Figure S4) were consistent with that observed in the 30 443 min interval study. On a broader level, the results also inform 444 the feasibility of utilizing this approach to construct the 445 pharmacokinetic profiles of xenobiotic compounds including 446 pharmaceutical drugs. As a complementary test, to evaluate the 447 THMP's ability to render an endogenous compound's 448 temporal profile, THMP-based fingertip sampling was 449 performed targeting lactate. Accordingly, one subject was 450 monitored at 30 min intervals in a sedentary state (where no 451 significant change in sweat lactate level was expected). The

results indicate that the sampled lactate by the THMP was 452 relatively stable over the duration of the test (Figure 2d), 453 validating the consistency of the analyte sampling capability of 454 the THMP.

THMP-Based Wireless Electrochemical Sensing Sys- 456 tem. With the THMP established as an effective sampling 457 reservoir, we next investigated its suitability as an electro- 458 chemical sensing medium. In that regard, one may need to 459 note that the electrochemical sensor response (which is 460 proportional to the target concentration in the hydrogel) must 461 be measured in relation to the hydrogel thickness to infer the 462 flux of the target molecules into the hydrogel reservoir. Here, 463 analyte sampling was performed with hydrogel micropatches of 464 three different thicknesses (340, 510, and 680  $\mu$ m, placed side 465 by side on a subject's fingertip). Lactate and caffeine were 466 targeted and quantified with the standard lab instruments. The 467 results show that for the tested sampling time (5 min), the 468 amount of target analytes sampled was relatively constant 469 among different thicknesses, implying the presence of a higher 470 analyte concentration in a thinner hydrogel (Figure S5), which, 471 in turn, relaxes the requirements for sensor sensitivity and limit 472

Based on these findings, the thinnest THMP (340  $\mu$ m thick) 474 was subsequently used to couple with an electrochemical 475 sensing system to noninvasively render sample-to-answer 476 biomarker data. As a proof-of-concept, we targeted lactate 477 with a custom-developed enzymatic sensing system (Figure 478 f3 3a). The lactate sensing module was composed of a THMP 479 f3 affixed upon a flexible PET substrate patterned with function- 480 alized Au electrodes (Figure 3b). The electrodes were 481 functionalized to implement a mediator-free electroenzymatic 482 sensing interface. 40,41 The structure of the working electrode 483 was composed of (1) a PVC layer interfacing the THMP, as a 484 diffusion-limiting membrane (to enhance the sensor dynamic 485 range); (2) a LOx layer, which generates hydrogen peroxide 486  $(H_2O_2)$ 

in proportion to the lactate concentration level in the 488 THMP; (3) a PPD layer, which mitigates the confounding 489 effect of electroactive species present in the sampled 490 perspiration (e.g., UA and AA); and (4) an MWCNT/PtNP 491 layer, which enhances the sensor sensitivity (leveraging the 492 nanostructure's high catalytic activity and large surface area). A 493 linear response of the developed sensing interface toward 494 lactate was observed over a range of 0-4 mM with the 495 sensitivity of 1.88  $\pm$  0.24  $\mu$ A/(mM cm<sup>2</sup>) and the LoD of 0.12 496  $\pm$  0.02 mM (Figure S6).

Calibration of this THMP-based sensing module was 498 performed with THMPs presoaked with lactate solutions 499 (with concentration levels in the range of 0-2 mM), displaying 500 a linear response with high repeatability (Figure 3c) and 501 indicating the suitability of the THMP interface for electro- 502 chemical sensing applications. Expanding on these findings, 503 selectivity tests were performed to verify the biofluid (as a 504 complex matrix) sensing capability of the THMP-sensor-505 coupled interface. To this end, the THMP-based lactate 506 sensing module was challenged against a diverse panel of 507 interfering species at physiologically relevant concentration 508 levels (including electrolytes, electroactive species, and other 509 small molecules). Figure 3d shows that the presence of each 510 nontargeted analyte has minimal response compared to that of 511 lactate. Furthermore, the sensor shows a negligible response to 512 the sequential introduction of those nontargeted analytes 513 (Figure S7). As shown in Figure S8, the sensor's biofluid 514

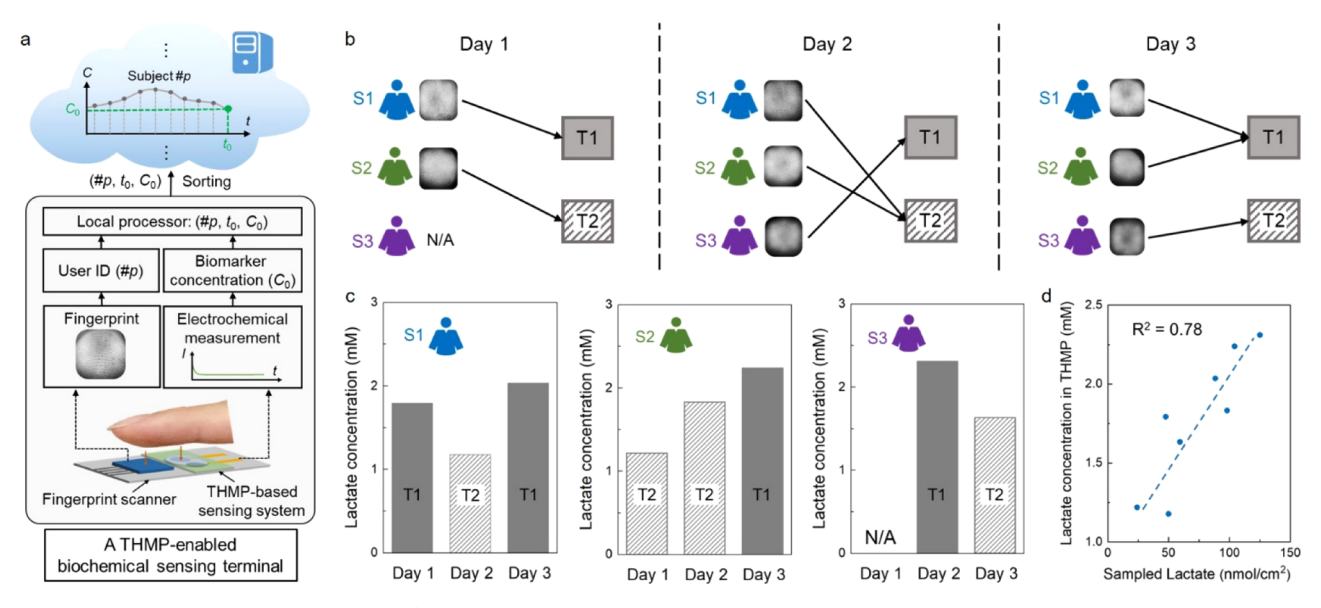


Figure 4. Terminal-based sensing network. (a) Schematic of the structure and function of a one-touch THMP-enabled biochemical sensing and user identification terminal. (b) Tracking sweat lactate among a group of three individuals (S1–S3) using two cloud-connected terminals (T1 and T2). Imaged fingerprints of each user entry are included, and each arrow indicates the terminal used by each subject (N/A indicates no entry by the subject). Photograph (right) shows a representative terminal. (c) Corresponding user-identified and sorted sweat lactate profiles of the users, rendered by the devised terminals. (d) Comparison of the in situ measured lactate concentration levels in THMP vs the corresponding amount of the sampled lactate measured by a lab instrument (YSI analyzer).

515 sample quantification capability was further validated by 516 comparing the estimated lactate concentration from the 517 developed sensor with that analyzed by a standard lab 518 instrument (YSI analyzer) toward a 10× diluted sweat 519 (mimicking the dilution of the sampled perspiration within 520 the THMP).

As an additional sensing performance parameter relevant to 521 522 the context at hand, the response time of the sensing module was characterized, which is dependent on the analyte diffusion dynamic (assuming operation in the diffusion-limited regime, 525 diffusion time  $\tau \propto H^2/D$ , where H is the diffusion length, or 526 the thickness of the THMP, and D is the analyte diffusion coefficient inside the hydrogel). Accordingly, a hydrogel was s28 mounted onto the sensor from t = 0 to 100 s, after which 1  $\mu$ L 529 of the concentrated sodium lactate (10 mM) sample was drop-530 cast onto hydrogel to mimic the natural perspiration 531 phenomenon. Hydrogels with different thicknesses 340, 510, s32 and 680  $\mu$ m were utilized to investigate the influence of 533 hydrogel thickness to the response time of the sensing module. 534 The sensing module's current response was monitored continuously, and the response time was defined and recorded 536 at the time corresponding to that where the sensor current response reached 90% of its maximum current change 537 (representative recording of the 340  $\mu$ m-thick hydrogel case is shown in Figure 3e). The measurements demonstrated that thinner hydrogels exhibited shorter response times, indicating the superior dynamic performance of a thin hydrogel (Figure 3e, inset). Considering the disposable nature of the THMPbased sensing module, the lifetime of the lactate sensor and the shelf life of THMP and sensor were investigated. Accordingly, 545 Figure S9 shows the continuous operation of the lactate sensor 546 for 4 h, demonstrating a sufficiently long lifetime of the 547 developed sensor. The shelf life of THMP and the lactate 548 sensor was characterized separately. To store THMP, a 549 hydrophobic plastic-based package was designed (Figure 550 \$10a, inset), which minimizes the water evaporation over

time. As shown in Figure S10a, less than a 10% weight loss of 551 THMP was observed after the storage of THMP within this 552 package for longer than 120 h at room temperature. In 553 addition, Figure S10b,c shows that the representative 554 characterized lactate sensors maintain their responsiveness 555 after 5 days of storage (at 4 °C). Future efforts with the 556 particular focus on preserving the enzyme activity can be 557 geared toward improving the shelf life.

To realize a fully integrated and self-sufficient biomarker 559 sampling and sensing system, the sensing module was 560 interfaced with a custom-developed Bluetooth-enabled readout 561 board, which implements seamless and in situ signal 562 acquisition, processing, and wireless transmission to a 563 dashboard (e.g., a mobile application; Figure 3f). At its core, 564 the board (Figure S11) functions as a potentiostat circuit, 565 consisting of biasing, amplification, and filtering stages, 566 controlled by an MCU. Prior to its deployment for on-body 567 biomarker measurements, the board's signal acquisition and 568 processing functionalities were validated by comparing its 569 readings against a commercial potentiostat for a range of 570 lactate concentration levels. Figure 3g shows a high level of 571 linearity between the board and potentiostat readouts. The 572 fully integrated sensing system was further validated by 573 demonstrating its ability to estimate the lactate level, sampled 574 directly from a subject's fingertip. Figure 3h demonstrates a 575 representative readout and the corresponding calibrated lactate 576 concentration level (raw recording is shown in the inset and is 577 compared to the readout of a blank THMP).

**Terminal-Based Sensing Network.** The noninvasive and 579 passive biomarker sampling and sensing nature of the THMP- 580 based wireless sensing system make it suitable for general 581 population monitoring, presenting a great potential for 582 incorporation within the IoT infrastructure. To this end, we 583 demonstrated a proof-of-concept for a distributed biochemical 584 sensing network, which can be modeled as an array of *k*-cloud- 585 connected terminals (each employing a THMP-based sensing 586

587 system), shared by *n* users. The terminals exploit the fingertip 588 as the sampling site, which uniquely allows for the 589 simultaneous collection of the user identification information 590 (from the fingerprint) and sweat biomarker information (from 591 natural perspiration). The capture of fingerprint information 592 allows individuals to take their biomarker reading with shared 593 terminals at different time points via exploiting the one-touch 594 biochemical sensing/user identification capability. In that 595 regard, user identification along with biomarker sensing 596 eliminates an extra step for the user intervention, allowing 597 for the convenient use of terminals for biomarker sampling.

As shown in Figure 4a, each terminal is composed of (1) an 599 identification module, which, at its core, employs a commercial 600 fingerprint scanner module and is configured to obtain the 601 fingerprint information from the top-half of the fingertip and 602 identify the corresponding user by comparing the imaged 603 fingerprint to a database of fingerprints, and (2) a THMP-604 based sensing system that captures the concentration of target 605 molecules from the lower half of the fingertip. Upon one-touch 606 information sampling, the biomarker information is paired with 607 the imaged fingerprint and linked to the user's identity at the 608 terminal level. Then, the user-identified and time-stamped 609 biomarker information is subsequently transmitted, with the 610 aid of a local processor, to cloud servers online, for information 611 sorting and updating the user's record. To assess the one-to-612 one mapping capability of the identification module, the user 613 identification based on the top-half of the fingertip (Figure 614 S12) was preliminarily characterized by creating a database of 615 20 index finger fingerprints from individual subjects and 616 verifying that the subsequently introduced partial fingerprints 617 were correctly identified (provided by the same group of 618 subjects). This result is aligned with the previous studies 619 demonstrating the robustness and accuracy in subject 620 identification based on partial fingerprint imaging. 42

Here, the proof-of-concept for the envisioned distributed biochemical sensing network was implemented to track lactate (123) (using the readily developed and described THMP-based (124) lactate sensing system) among a group of three individuals (125) and two cloud-(126) connected terminals (127) via a cellular module, k=2). Over a (127) period of 3 days, these individuals were instructed to use the (128) terminal, depending on their convenience and availability. A (129) database of their index finger fingerprints was created and (130) loaded onto the fingerprint scanner module of each of the (131) terminals to allow for tracking the user entries. The recorded (132) entries confirmed that Subjects 1 and 2 provided one sample (133) per day, and Subject 3 only used the terminal on the second (134) and third day (Figure 4b).

For each entry, the electrochemically generated sensor response was postcalibrated, user-identified, time-stamped, and then transmitted to a custom-developed Google Cloud platform. The uploaded data are sorted according to the existing user ID database, yielding the sweat lactate profiles of each individual (Figure 4c). To validate the lactate readings, analytes sampled in the THMP were extracted into acetate buffer solutions after each electrochemical measurement, and the lactate concentration levels were quantified by the tommercial lab instrument (YSI analyzer). Quantification by the YSI analyzer before and after amperometric measurement indicated that the electrochemical measurement process had minimal influence on the lactate present (Figure S13). Figure 4d shows that the calibrated concentration levels obtained from the THMP-based sensing system and the corresponding

amount of the sampled lactate quantified by the lab instrument 650 reading are correlated ( $R^2 = 0.78$ ). The results indicate that the 651 devised sensing terminal can capture the trend of the sampled 652 lactate amount variation. It is also worth noting that the 653 nonideal characteristics in the measurements (e.g., finite x/y- 654 axis intercept, inconsistent relative change between some of the 655 pairs of measurements) may be related to the fact that (1) the 656 measurement of YSI in the low-concentration regime is prone 657 to error and (2) a small portion of the sampled analyte may 658 stay on the THMP surface and may not diffuse into the bulk 659 hydrogel. To this end, system-level calibration can be 660 incorporated to correct such nonideal characteristics.

On a broader level, the subject-independent and terminal- 662 based nature of the demonstrated network allows for the 663 integration of other sensors and automated back-end 664 processing modules (including sample preparation and 665 calibration units) to target a wide panel of biomarkers.

### CONCLUSIONS AND OUTLOOK

In conclusion, a thin hydrogel micropatch was devised for 668 simultaneous natural perspiration collection and in situ 669 electrochemical analysis. A first-order fluidic model was used 670 to describe the enhanced analyte collection capability of the 671 hydrogel, a property that was verified through caffeine and 672 lactate sampling. Informed by the biomarker sampling 673 characterization results across different body locations, the 674 fingertip was determined as the optimal site for natural 675 perspiration sampling, which was subsequently used to 676 demonstrate the successful tracking of the dosage level and 677 metabolic pattern of the caffeine intake among different 678 subjects. The suitability of THMP as an electrochemical 679 sensing medium was characterized by augmenting the THMP 680 with a wireless enzymatic lactate sensing module, for which 681 excellent reproducibility, selectivity, and response time ~50 s 682 were demonstrated. These results inform the utility of natural- 683 perspiration-based biomarker analysis, which can create new 684 directions for noninvasive chemo/biosensing. To reinforce this 685 point, we demonstrated the proof-of-concept for an 686 unprecedented distributed terminal-based bio/chemical sensor 687 network, which uniquely capitalizes on the fingertip as a site for 688 simultaneous biomarker data sampling (via natural perspi- 689 ration) and user identification (via fingerprint).

Future work will focus on utilizing and building upon the 691 presented technology to characterize and address relevant 692 confounding factors (that, at the current stage, remain 693 underexplored, because of the lack of suitable technologies 694 to perform such studies) toward establishing the physiologi- 695 cally meaningful interpretation of the biomarker readings. In 696 that regard, future engineering efforts will involve the 697 incorporation of a perspiration rate sensing interface to 698 normalize the THMP-based biomarker readings in relation 699 to the perspiration rate, mitigating the confounding effects of 700 inter/intrasubject perspiration rate variability (assuming a 701 direct measure of the analyte concentration in sweat is 702 needed). Also, a standard skin surface cleaning component in 703 the chemo/biosensing terminal will be devised to achieve 704 autonomous operation and to minimize skin contamination. 705 Furthermore, large-scale clinical investigations will be 706 performed to systematically characterize the contribution of 707 relevant underlying biological sources (e.g., natural perspi- 708 ration, sweat gland/skin metabolism, transepithelial water loss) 709 and understand the corresponding analyte partitioning path- 710 ways, to establish the physiological significance of the 711

712 biomarker readings (e.g., correlation with blood concentration 713 levels) for the context at hand. The joint engineering and 714 clinical efforts will converge to realize a scalable network with 715 fully automated bioanalytical capabilities to render physiolog-716 ically relevant information. The presented noninvasive chemo/717 biosensing network can be positioned within the IoT 718 infrastructure, widening the accessibility of personalized health 719 monitoring for the general population.

## **ASSOCIATED CONTENT**

## S Supporting Information

722 The Supporting Information is available free of charge on the 723 ACS Publications website at DOI: 10.1021/acssen-724 sors.9b01727.

Schematic of THMP array fabrication; sampled lactate with different collection procedure; LC-MS/MS for caffeine quantification; caffeine sampling from three subjects at 1 h intervals; relationship of hydrogel thickness and amount of analyte sampled, and the corresponding analyte concentration within the hydrogel; calibration curves of three representative lactate sensors; selectivity of lactate sensor; validation of diluted sweat measurement; lifetime of lactate sensor; long-time storage of THMP-based sensing module; readout circuitry used in THMP-based sensing system; finger-print information acquisition from the top-half of the fingertip; influence of electrochemical measurement to the lactate concentration in THMP (PDF)

Natural perspiration on the fingertip of a subject (MOV)

### AUTHOR INFORMATION

#### 741 Corresponding Author

742 \*E-mail: emaminejad@ucla.edu.

743 **ORCID** ®

726

727

728

729

730

731

732

733

734

735

736

737

738

739

744 Shuyu Lin: 0000-0002-5248-6124 745 Bo Wang: 0000-0002-3986-3415 746 Dino Di Carlo: 0000-0003-3942-4284

#### 747 Author Contributions

748 S.L. and B.W. contributed equally. S.L., B.W., and S.E. 749 conceived the idea and designed the experiments; S.L. led 750 the experiments (with assistance from B.W., Y.Z., R.S., X.C., 751 W.Y., H.H., H.L., C.H., D.L., J.T., Y.C., D.D.C., C.M., and 752 S.E.); Y.Z. and X.C. led the sensor fabrication; W.Y. and H.H. 753 led PCB and system design; S.L., B.W., R.S., Y.Z., X.C., W.Y., 754 H.H., H.L., Y.C., D.D.C, C.M., and S.E. contributed to data 755 analysis and interpretation; S.L., B.W., R.S., X.C., W.Y., H.H., 756 Y.C., D.D.C., C.M., and S.E. drafted the manuscript, and all 757 authors provided feedback. S.E. supervised the study.

758 Notes

759 The authors declare no competing financial interest.

# **MACKNOWLEDGMENTS**

761 This work was supported by the S.E.'s startup package 762 provided by the UCLA Henry Samueli School of Engineering 763 and Applied Sciences. Components of research are supported 764 by the National Science Foundation (Award #1722972), 765 Stanford Genome Technology Center Distinguished Young 766 Investigator Award (in partnership with Intermountain 767 Healthcare), PhRMA Foundation (Research Starter Grant in 768 Translational Medicine and Therapeutics), and the funding 769 secured by the Preservation of the Force and Family Program

at US Special Operations Command (executed as a subaward 770 issued to the University of California at Los Angeles by the 771 Henry M. Jackson Foundation under a cooperative agreement 772 with the Uniformed Services University). The authors 773 appreciate UCLA nanoelectronics research facility (NRF) for 774 their help in device fabrication/characterization. The authors 775 also thank Christopher Yeung, Zhaoqing Wang, Kayla Choi, 776 Sina Moshfeghi, Phoenix Stout, Jonghwee Park, Dinhan Pham, 777 and Shuxin Tan for their assistance with device testing and 778 system design. R.S. acknowledges support from the UCLA- 779 Caltech Medical Scientist Training Program (NIGMS T32 780 GM008042).

#### REFERENCES

(1) Byrne, R.; Diamond, D. Chemo/bio-sensor networks. *Nat.* 783 *Mater.* **2006**, *5*, 421–424.

782

(2) Lin, H.; Zhao, Y.; Lin, S.; Wang, B.; Yeung, C.; Cheng, X.; Wang, 785 Z.; Cai, T.; Yu, W.; King, K.; Tan, J.; Salahi, K.; Hojaiji, H.; 786 Emaminejad, S. A rapid and low-cost fabrication and integration 787 scheme to render 3D microfluidic architectures for wearable biofluid 788 sampling, manipulation, and sensing. *Lab Chip* 2019, 19, 2844–2853. 789

(3) Lin, H.; Hojaiji, H.; Lin, S.; Yeung, C.; Zhao, Y.; Wang, B.; 790 Malige, M.; Wang, Y.; King, K.; Yu, W.; Tan, J.; Wang, Z.; Cheng, X.; 791 Emaminejad, S. A wearable electrofluidic actuation system. *Lab Chip* 792 **2019**, 19, 2966–2972.

(4) Heikenfeld, J.; Jajack, A.; Rogers, J.; Gutruf, P.; Tian, L.; Pan, T.; 794 Li, R.; Khine, M.; Kim, J.; Wang, J.; et al. Wearable sensors: 795 modalities, challenges, and prospects. *Lab Chip* **2018**, *18*, 217–248. 796 (5) Lee, H.; Choi, T. K.; Lee, Y. B.; Cho, H. R.; Ghaffari, R.; Wang, 797

L.; Choi, H. J.; Chung, T. D.; Lu, N. S.; Hyeon, T.; Choi, S. H.; Kim, 798 D. H. A graphene-based electrochemical device with thermores-799 ponsive microneedles for diabetes monitoring and therapy. *Nat.* 800 *Nanotechnol.* **2016**, *11*, 566–572.

(6) Koh, A.; Kang, D.; Xue, Y.; Lee, S.; Pielak, R. M.; Kim, J.; 802 Hwang, T.; Min, S.; Banks, A.; Bastien, P.; Manco, M. C.; Wang, L.; 803 Ammann, K. R.; Jang, K. I.; Won, P.; Han, S.; Ghaffari, R.; Paik, U.; 804 Slepian, M. J.; Balooch, G.; Huang, Y. G.; Rogers, J. A. A soft, 805 wearable microfluidic device for the capture, storage, and colorimetric 806 sensing of sweat. *Sci. Transl. Med.* **2016**, 8, No. 366ra165.

(7) Bariya, M.; Nyein, H. Y. Y.; Javey, A. Wearable sweat sensors. 808 Nat. Electron. 2018, 1, 160–171.

(8) Heikenfeld, J. Non-invasive Analyte Access and Sensing through 810 Eccrine Sweat: Challenges and Outlook circa 2016. *Electroanalysis* 811 **2016**, 28, 1242–1249.

(9) Martín, A.; Kim, J.; Kurniawan, J. F.; Sempionatto, J. R.; Moreto, 813 J. R.; Tang, G. D.; Campbell, A. S.; Shin, A.; Lee, M. Y.; Liu, X. F.; 814 Wang, J. Epidermal Microfluidic Electrochemical Detection System: 815 Enhanced Sweat Sampling and Metabolite Detection. ACS Sens. 2017, 816 2, 1860–1868.

(10) Gao, W.; Emaminejad, S.; Nyein, H. Y. Y.; Challa, S.; Chen, K. 818 V.; Peck, A.; Fahad, H. M.; Ota, H.; Shiraki, H.; Kiriya, D.; Lien, D. 819 H.; Brooks, G. A.; Davis, R. W.; Javey, A. Fully integrated wearable 820 sensor arrays for multiplexed in situ perspiration analysis. *Nature* 821 **2016**, 529, 509–514.

(11) Zhang, Y.; Guo, H. X.; Kim, S. B.; Wu, Y. X.; Ostojich, D.; Park, 823 S. H.; Wang, X. J.; Weng, Z. Y.; Li, R.; Bandodkar, A. J.; Sekine, Y.; 824 Choi, J.; Xu, S.; Quaggin, S.; Ghaffari, R.; Rogers, J. A. Passive sweat 825 collection and colorimetric analysis of biomarkers relevant to kidney 826 disorders using a soft microfluidic system. *Lab Chip* **2019**, *19*, 1545—827 1555.

(12) Simmers, P.; Li, S. K.; Kasting, G.; Heikenfeld, J. Prolonged and 829 localized sweat stimulation by iontophoretic delivery of the slowly- 830 metabolized cholinergic agent carbachol. *J. Dermatol. Sci.* **2018**, 89, 831 40–51.

(13) Emaminejad, S.; Gao, W.; Wu, E.; Davies, Z. A.; Nyein, H. Y. 833 Y.; Challa, S.; Ryan, S. P.; Fahad, H. M.; Chen, K.; Shahpar, Z.; 834 Talebi, S.; Milla, C.; Javey, A.; Davis, R. W. Autonomous sweat 835 extraction and analysis applied to cystic fibrosis and glucose 836

DOI: 10.1021/acssensors.9b01727 ACS Sens. XXXX, XXX, XXX—XXX

I

837 monitoring using a fully integrated wearable platform. *Proc. Natl.* 838 *Acad. Sci. U.S.A.* **2017**, *114*, 4625–4630.

- 839 (14) Kim, J.; Campbell, A. S.; de Avila, B. E. F.; Wang, J. Wearable 840 biosensors for healthcare monitoring. *Nat. Biotechnol.* **2019**, 37, 389—841 406.
- 842 (15) Jajack, A.; Brothers, M.; Kasting, G.; Heikenfeld, J. Enhancing 843 glucose flux into sweat by increasing paracellular permeability of the 844 sweat gland. *PLoS One* **2018**, *13*, No. e0200009.
- 845 (16) Sonner, Z.; Wilder, E.; Heikenfeld, J.; Kasting, G.; Beyette, F.; 846 Swaile, D.; Sherman, F.; Joyce, J.; Hagen, J.; Kelley-Loughnane, N.; 847 Naik, R. The microfluidics of the eccrine sweat gland, including 848 biomarker partitioning, transport, and biosensing implications. 849 *Biomicrofluidics* 2015, 9, No. 031301.
- 850 (17) Leggett, R.; Lee-Smith, E. E.; Jickells, S. M.; Russell, D. A. 851 "Intelligent" fingerprinting: Simultaneous identification of drug 852 metabolites and individuals by using antibody-functionalized nano-853 particles. *Angew. Chem., Int. Ed.* 2007, 46, 4100–4103.
- 854 (18) Hazarika, P.; Russell, D. A. Advances in Fingerprint Analysis. 855 Angew. Chem., Int. Ed. **2012**, *51*, 3524–3531.
- 856 (19) Costa, C.; Webb, R.; Palitsin, V.; Ismail, M.; de Puit, M.; 857 Atkinson, S.; Bailey, M. J. Rapid, Secure Drug Testing Using 858 Fingerprint Development and Paper Spray Mass Spectrometry. *Clin.* 859 *Chem.* **2017**, *63*, 1745–1752.
- 860 (20) Burns, M.; Baselt, R. C. Monitoring drug use with a sweat 861 patch: an experiment with cocaine. *J. Anal. Toxicol.* **1995**, *19*, 41–48.
- 862 (21) Dolan, K.; Rouen, D.; Kimber, J. An overview of the use of 863 urine, hair, sweat and saliva to detect drug use. *Drug Alcohol Rev.* 864 **2004**, 23, 213–217.
- 865 (22) Dutkiewicz, E. P.; Lin, J. D.; Tseng, T. W.; Wang, Y. S.; Urban, 866 P. L. Hydrogel Micropatches for Sampling and Profiling Skin 867 Metabolites. *Anal. Chem.* **2014**, *86*, 2337–2344.
- 868 (23) Dutkiewicz, E. P.; Chiu, H. Y.; Urban, P. L. Micropatch-arrayed 869 pads for non-invasive spatial and temporal profiling of topical drugs 870 on skin surface. *J. Mass Spectrom.* **2015**, *50*, 1321–1325.
- 871 (24) Kuwayama, K.; Tsujikawa, K.; Miyaguchi, H.; Kanamori, T.; 872 Iwata, Y. T.; Inoue, H. Time-course measurements of caffeine and its 873 metabolites extracted from fingertips after coffee intake: a preliminary 874 study for the detection of drugs from fingerprints. *Anal. Bioanal.* 875 *Chem.* 2013, 405, 3945–3952.
- 876 (25) Nagamine, K.; Mano, T.; Nomura, A.; Ichimura, Y.; Izawa, R.; 877 Furusawa, H.; Matsui, H.; Kumaki, D.; Tokito, S. Noninvasive Sweat-878 Lactate Biosensor Emplsoying a Hydrogel-Based Touch Pad. *Sci. Rep.* 879 **2019**, *9*, No. 10102.
- 880 (26) Schmidt, B.; Roberts, R. S.; Davis, P.; Doyle, L. W.; Barrington, 881 K. J.; Ohlsson, A.; Solimano, A.; Tin, W. Caffeine Apnea Prematurity 882 Trial, G. Caffeine therapy for apnea of prematurity. *N. Engl. J. Med.* 883 **2006**, 354, 2112–2121.
- 884 (27) Dobson, N. R.; Liu, X. X.; Rhein, L. M.; Darnall, R. A.; Corwin, 885 M. J.; McEntire, B. L.; Ward, R. M.; James, L. P.; Sherwin, C. M. T.; 886 Heeren, T. C.; Hunt, C. E. Salivary caffeine concentrations are 887 comparable to plasma concentrations in preterm infants receiving 888 extended caffeine therapy. *Br. J. Clin. Pharmacol.* **2016**, 82, 754–761.
- 889 (28) Derbyshire, P. J.; Barr, H.; Davis, F.; Higson, S. P. J. Lactate in 890 human sweat: a critical review of research to the present day. *J. Physiol. Sci.* **2012**, *62*, 429–440.
- 892 (29) Jia, W.; Bandodkar, A. J.; Valdes-Ramirez, G.; Windmiller, J. R.; 893 Yang, Z. J.; Ramirez, J.; Chan, G.; Wang, J. Electrochemical Tattoo 894 Biosensors for Real-Time Noninvasive Lactate Monitoring in Human 895 Perspiration. *Anal. Chem.* **2013**, *85*, 6553–6560.
- 896 (30) Khodagholy, D.; Curto, V. F.; Fraser, K. J.; Gurfinkel, M.; 897 Byrne, R.; Diamond, D.; Malliaras, G. G.; Benito-Lopez, F.; Owens, R. 898 M. Organic electrochemical transistor incorporating an ionogel as a 899 solid state electrolyte for lactate sensing. *J. Mater. Chem.* **2012**, 22, 900 4440–4443.
- 901 (31) Tai, L. C.; Gao, W.; Chao, M. H.; Bariya, M.; Ngo, Q. P.; 902 Shahpar, Z.; Nyein, H. Y. Y.; Park, H.; Sun, J.; Jung, Y.; Wu, E.; Fahad, 903 H. M.; Lien, D. H.; Ota, H.; Cho, G.; Javey, A. Methylxanthine Drug 904 Monitoring with Wearable Sweat Sensors. *Adv. Mater.* **2018**, *30*, 905 No. 1707442.

- (32) Ismail, M.; Stevenson, D.; Costa, C.; Webb, R.; de Puit, M.; 906 Bailey, M. Noninvasive Detection of Cocaine and Heroin Use with 907 Single Fingerprints: Determination of an Environmental Cutoff. Clin. 908 Chem. 2018, 64, 909–917.
- (33) Ohshima, Y.; Shimizu, H.; Yanagishita, T.; Watanabe, D.; 910 Tamada, Y.; Sugenoya, J.; Tsuda, T.; Matsumoto, Y. Changes in Na+, 911 K+ concentrations in perspiration and perspiration volume with 912 alternating current iontophoresis in palmoplantar hyperhidrosis 913 patients. *Arch. Dermatol. Res.* **2008**, 300, 595–600.
- (34) Kim, J.; Farahmand, M.; Dunn, C.; Davies, Z.; Frisbee, E.; 915 Milla, C.; Wine, J. J. Evaporimeter and bubble-imaging measures of 916 sweat gland secretion rates. *PLoS One* **2016**, *11*, No. e0165254.
- (35) Heikenfeld, J.; Jajack, A.; Feldman, B.; Granger, S. W.; 918 Gaitonde, S.; Begtrup, G.; Katchman, B. A. Accessing analytes in 919 biofluids for peripheral biochemical monitoring. *Nat. Biotechnol.* **2019**, 920 37, 407–419.
- (36) Ptolemy, A. S.; Tzioumis, E.; Thomke, A.; Rifai, S.; Kellogg, M. 922 Quantification of theobromine and caffeine in saliva, plasma and urine 923 via liquid chromatography-tandem mass spectrometry: A single 924 analytical protocol applicable to cocoa intervention studies. *J.* 925 *Chromatogr. B* **2010**, 878, 409–416.
- (37) Zhang, Y.; Mehrotra, N.; Budha, N. R.; Christensen, M. L.; 927 Meibohm, B. A tandem mass spectrometry assay for the simultaneous 928 determination of acetaminophen, caffeine, phenytoin, ranitidine, and 929 theophylline in small volume pediatric plasma specimens. *Clin. Chim.* 930 *Acta* 2008, 398, 105–112.
- (38) Taylor, N. A.; Machado-Moreira, C. A. Regional variations in 932 transepidermal water loss, eccrine sweat gland density, sweat secretion 933 rates and electrolyte composition in resting and exercising humans. 934 Extreme Physiol. Med. 2013, 2, No. 4.
- (39) Fruhstorfer, H.; Abel, U.; Garthe, C. D.; Knuttel, A. Thickness 936 of the stratum corneum of the volar fingertips. *Clin. Anat.* **2000**, *13*, 937 429–433.
- (40) Wen, X.; Wang, B.; Huang, S.; Liu, T.; Lee, M. S.; Chung, P. S.; 939 Chow, Y. T.; Huang, L. W.; Monbouquette, H. G.; Maidment, N. T.; 940 Chiou, P. Y. Flexible, multifunctional neural probe with liquid metal 941 enabled, ultra-large tunable stiffness for deep-brain chemical sensing 942 and agent delivery. *Biosens. Bioelectron.* **2019**, *131*, 37–45.
- (41) Wang, B.; Koo, B.; Huang, L. W.; Monbouquette, H. G. 944 Microbiosensor fabrication by polydimethylsiloxane stamping for 945 combined sensing of glucose and choline. *Analyst* **2018**, *143*, 5008–946 5013.
- (42) Jea, T. Y.; Chavan, V. S.; Govindaraju, V.; Schneider, J. K. 948 Security and Matching of Partial Fingerprint Recognition Systems, In 949 Biometric Technology for Human Identification, Proceedings of SPIE, 950 2004; pp 39–50.